24 th EUROPEAN ROTORCRAFT FORUM
Marseilles, France-15th-17th September 1998

FM02

Comparison of the Flight Dynamics of Equivalent Tilt Rotor and Tilt Wing Configurations

Binoy J Manimala and Roy Bradley
Department of Mathematics,
Glasgow Caledonian University,
Glasgow

Tilt rotor and the tilt wing are two of the successful V/STOL aircraft concepts. This paper describes a basic mathematical modelof a tilt wing aircraft for simulation modelling and a comparativeflight dynamics, analysis with an equivalent tilt rotor configuration. For comparison the tilt wing aircraft is assumed to have the same aerodynamic and physical characteristics of the XV-15 tilt rotor. Also discussed is the adaptation of an inverse simulation technique originally, developed for helicopter handling qualities into tilt wing modelling. The inverse simulation technique is used to evaluate the ability of the tilt wing aircraft to perform a set of precisely defined longitudinal and lateral manoeuvres.

Nomenclature

$\mathbf{u}$	Control state vector
V_f	Fight speed
$\mathbf{X}$	Vehicle state vector
x_e, y_e, z_e	Displacement with respect to the earth fixed inertial frame
$\mathbf{Y}$	Output vector
β	Vehicle side slip angle
γ	Rotor shaft tilt angle measured from the vertical position
γ_f	Vehicle climb angle
Ω	Vehicle turn rate
ϕ	Vehicle bank attitude
θ	Vehicle pitch attitude
θ_{1cc}	Combined lateral cyclic input
θ_{0c}, θ_{0d}	Combined and differential Collective input.
θ_{1sc}, θ_{1sd}	Combined and differential longitudinal input

1 Introduction

The objective of the work described in this paper is to establish a simulation platform for a comparative investigation of the flight dynamics of tilt rotor and tilt wing aircraft. The simulation environment contains state of the art algorithms for trim, stability analysis, and manoeuvre guidance to enable a quantitative comparison of the two configurations with the ultimate aim of achieving such a comparison in helicopter mode, aeroplane mode and throughout the conversion mode. The paper describes, with up to date results, the achievements to date. First, in section 2, some background on the development of the two configurations is presented and the tilt rotor modelling by McVicar and Bradley [1] recalled as a context for the subsequent development. Section 3 sets out the modelling framework for the simulation with careful attention to its potential for generalisation and also to its limitations. Section 4 examines the comparative trim problem for the two vehicle, presenting the detailed algorithm. The manoeuvre guidance capability of the aircraft is dealt in section 5. The helicopter inverse simulation method of Rutherford

and Thomson [2] is developed for this special application and a range of manoeuvre definitions established and simulated for a comparative study of the ideal pilot's control strategy. A comparative flight mechanics analysis of the tilt rotor and tilt wing configurations in hover and conversion modes is performed in section 6. Finally in the paper the planned future developments are addressed and conclusions drawn about the whole programme.

2 Background

Over the past 50 years, the attempts to combine the vertical take off and landing capability of a helicopter with the high forward speed of a conventional fixed wing resulted in a new category of aircraft called the Vertical /Short Take Off and Landing (V/STOL) aircraft. Two successful concepts were the Tilt Rotor and the Tilt Wing aircraft. The tilt rotor comprises a conventional wing and fuselage assembly with two large prop rotors mounted on nacelles at each wing tip. The plane of the prop rotors may be tilted from the vertical (helicopter mode) to the horizontal (aeroplane mode) during a transition phase. This property enables the tilt rotor to hover, take-off and land like a helicopter and to fly like a conventional aircraft on medium and long distance journeys. The tilt rotor concept has been in existence since the early 1950s and the major experimental programmes started at Bell Helicopter with the XV-3 which culminated in successful flight testing. Bell subsequently went on to develop the more successful XV-15 which proved the practicality of the tilt-rotor concept and led, in partnership with Boeing to the military V-22 Osprey programme.

The tilt-wing offers a similar solution to the V/STOL concept by tilting the entire wing in line with engine and the rotors. This provides the benefit of better aerodynamic flow characteristics over the wing and the control surfaces during the transition phase. Tilt-wing aircraft have little loss of lift compared to a tilt-rotor due to down wash of air from the rotors onto the wing. The main disadvantages of a tilt-wing aircraft over a tilt-rotor aircraft is the high angle of attack of the wing during the hover and conversion flights. Control of the aircraft in hover especially during gusts is difficult. The history of the tilt-wing concept started in the late 1950s with Vertol VZ-2 which made a successful transition from hovering to forward flight in 1958 [3]. The Hillier-Vought XC-142A and Candair CL-84 are two of the notable tilt-wing aircraft that have proved the concept viability through flight test programmes. Currently, a civil tilt-wing project is being pursued by the Ishida Aerospace Research Inc. who hope to have their TW-68 tilt-wing [4] certified by the end of the decade.

It is apparent that the tilt rotor and tilt wing concepts both represents elegant solutions to the problem of V/STOL applications. However, a key question that remains to be analysed in detail is which configurations represents the better solution in terms of aerodynamic, structural, operational, reliability and cost considerations. Chana and Sullivan [5] detail the advantages of a tilt-wing aircraft over a tilt-rotor in terms of structural, operational, cost and reliability aspects. The scope of this work is however, limited to an aerodynamic performance analysis alone between the two configurations.

A generic flight dynamics real time simulation model of the tilt rotor configuration was effectively modelled by McVicar [1], who developed novel trim and stability analysis and demonstrated them on a XV15 for which a measure of comparative data existed for validation. Simple transitions from helicopter to aeroplane mode were demonstrated for a trim-map approach to manoeuvre control. There is a natural development from this work to consider more sophisticated manoeuvre control, bearing in mind the nature of likely operations of the vehicle and a natural curiosity to compare the configuration with a partner tilt wing to assess their comparative control and performance behaviour. Comparison of two configurations can be best achieved by two aircraft of similar size and aerodynamic characteristics. All the tilt wing aircraft that have been built and flown were used propellers whereas the XV-15 tilt rotor used large prop-rotors and rotor controls. Due to the unavailability of any aerodynamic data for a tilt wing aircraft of the XV-15 class it was decided that a direct comparison can be best made by adopting the XV-15 configuration for the tilt wing. This meant that the tilt wing model have the same control mechanism and other characteristics of the XV-15 aircraft enabling a direct comparison of the two concepts.

3 Overview of the Tilt Wing Mathematical Model

3.1 Rotor Modelling

The blade geometry of a prop-rotor compared to a helicopter rotor blade is complex due to the high twist and chord variation from root to tip.

Also, high rotational speed of a prop-rotor causes the blade elements (towards the tip) to operate at speeds where compressibility effects have an important influence on the lift and drag coefficients of the rotor blades. Hence an individual blade formulation using blade element theory rather than a quasi-steady disc model is used to derive the rotor loads. In blade element theory, a blade is divided into several blade elements with each treated as a lifting surface. The rotor forces and moments are obtained by integrating the forces and moments produced by the blade elements over the span of the blade. The blade flapping equation is derived from the centre spring model [6]. The centre spring model assumes the rotor blade to be a cantilever hinged at the blade hub with the flapping motion of the blade resisted by the spring stiffness at the hub. Lagging and feathering motions of the blades are considered to be of less significance and not included in this analysis. Also, couplings from lagging and feathering motions into the flap dynamics are ignored. Rotor down wash is modelled using Peters-HaQuang inflow model [7]. This is an unsteady wake model which take into account of the time delay of the large mass of air flowing through the rotor disc and the effect of dynamic changes in pitching and rolling moment of the rotor disc on the inflow distribution.

3.2 Wing and Other Aerodynamic Components

The wing is treated in four segments, with the outer left and right sections immersed in the rotor slip stream. The free stream velocities at any

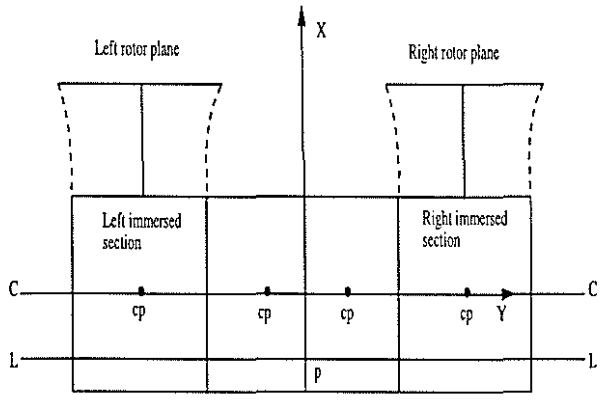

Figure 1: Wing modelling

two points in the wing are not, in general, the same. However, in flight mechanics studies it is usually sufficient to compute the velocity at the aerodynamic centre of pressure and assume it to be the same at every point of the wing section. The aerodynamic forces and moments acting on these wing sections are calculated separately using the free stream velocities at the centre of pressure and added together to get the total force and moment generated by the wing. The velocity at the unimmersed sections are calculated by summing the velocities due to angular(roll, pitch and yaw motions) and linear motions of the aircraft.

In tilt wing aircraft, the impingement of rotor slip stream on the wing is an important factor to be taken into account-especially in helicopter and conversion mode flights. In fact, most of the tilt wing aircraft used rotor slip stream as a source of yaw control in helicopter and transition mode flights. This was achieved by the differential usage of ailerons on the left and right sections of the wing which are immersed in the rotor wake. The effect of rotor wake on the wing is less significant in aircraft mode due to the fact that the value of induced velocity is considerably less when the vehicle is speeding forward with the wings tilted to horizontal position. However, rotor wake impingement on the wing has been implemented in this work at all wing angles by super imposing the uniform component of the induced velocity onto the vehicle free stream velocity. One of the key assumption of this analysis is that rotor slip stream travels parallel to the rotor shaft with no deflection of the flow due to vehicle velocity. The region of the wing immersed in the rotor wake is taken to be the rectangular area directly below the rotor(see Figure 1). The width of the rectangle is assumed to depend on slip stream contraction factor which is expressed as a function of thrust coefficient and the distance of the wing centre from the rotor hub. The aerodynamic lift and drag coefficients are defined in look-up tables for angle of attack varying from 0 to 360 degrees for different flap settings.

The horizontal stabiliser, vertical fin and the fuselage are modelled in the same manner as that of the wing using aerodynamic look-up tables for different settings of rudder (for vertical fin lift and drag) and elevator (for horizontal stabiliser lift and drag). The rotor up wash on the horizontal stabiliser is modelled using wind tunnel data. All the aerodynamic data used are adopted from reference [9] where they were used for the real time simulation of the XV-15 tilt-rotor aircraft.

3.3 Other Factors in the Mathematical Model

The effect of wing tilt on the centre of gravity changes are included in the model. There is no

engine model and hence constant engine speed is assumed

4 Partial Periodic Trim Algorithm

The trim problem seeks for the control inputs required to keep the aircraft in a prescribed equilibrium position. The equilibrium position may be turning, slide slipping, climbing or descending flight, but the general condition for trim is that the rate of change of the state vector is zero for some value of the control vector **u**. Therefore, the trimmed control vector is obtained by setting the acceleration terms in the equation of motion to zero and iterating for the control displacements until the prescribed flight conditions are reached. The vehicle states obtained through the trimming strategy above will adopt constant state values in trim only if the aerodynamic forces and moments generated are constant. This method is only adequate when a quasi steady rotor disc model is adopted for the rotor modelling. In this work the rotor model is based on individual blade co-ordinates and hence the aerodynamic forces and moments generated by the rotor will be essentially periodic. Since the equations of motion reflect any periodicity of the forcing terms, the trim solution adopts periodic states. Therefore, when seeking the trim solution it is necessary to look for a periodic solution to the equations of motion with the prescribed flight condition adopting the mean values over the period considered.

McVicar and Bradley developed a trimmed algorithm which is capable of obtaining periodic trim states and the required control states for a specified set of mean flight paths. The algorithm also made use of the symmetry of the rotor to minimise computational time. The algorithm was called the Partial Periodic Trimming Algorithm(PPTA) and the details can be obtained from reference [8]. The PPTA was successfully implemented in tiltrotor and conventional helicopter simulation models and the trim solutions obtained were found to be of high quality which were precisely maintained throughout for long periods of forward simulation. An overview of the Partial Periodic Trimming Algorithm along with the definitions of control and flight path vectors is given below.

4.1 Controls in helicopter and conversion mode flights

In helicopter and conversion mode flights there are five control states available to the pilot which provide the control authority as summarised in Table 1 and illustrated in Figure 2. The five rotor con-

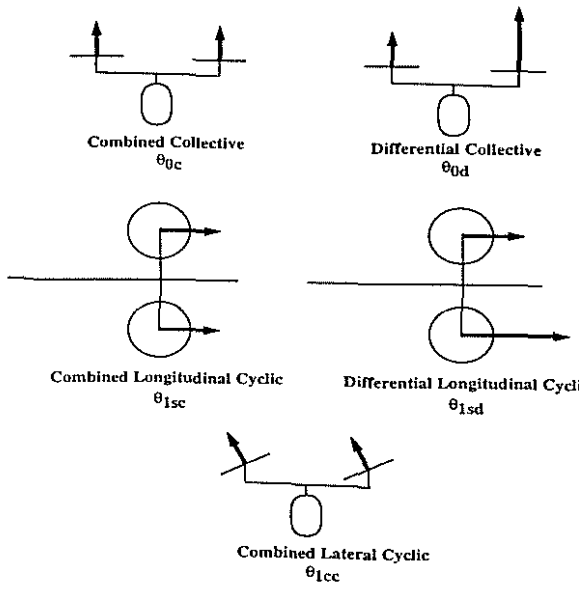

Figure 2: Controls in helicopter and conversion mode flight

Table 1: Rotor Controls

Axis	Rotor Control
Pitch	Combined Longitudinal Cyclic(θ_{1sc})
Roll	Differential Collective (θ_{0d}) + Combined Lateral Cyclic (θ_{1cc})
Yaw	Differential Longitudinal Cyclic (θ_{1sd})
Heave	Combined Collective (θ_{0c})

trol states are obtained from pilot stick displacements through gearing laws expressed as look up tables(see reference [9] for details). The rotor controls exerts maximum authority in the helicopter mode flight. The controls are washed out through functions of rotor shaft tilt angle as the aircraft converts to the aeroplane mode, transferring the control authority to the conventional aerodynamic control surfaces viz., ailerons, rudder and elevator.

4.2 Flight path definitions

Five rotor control states are arranged in the following order to form the control vector **u** :-

$$\mathbf{u} = [\ \theta_{0c}\ \ \theta_{0d}\ \ \theta_{1sc}\ \ \theta_{1sd}\ \ \theta_{1cc}\ ]^T$$

Since there are five control states, as many flight paths(or trim conditions) can also be specified. The

choice of the flight paths in this work is given below:

$$\mathbf{x} = [\ V_f \ \ \beta \ \ \gamma_f \ \ \Omega \ \ \phi\ ]^T$$

where,

V_f	-	flight speed
β	-	vehicle side slip angle
γ_f	-	vehicle climb angle
Ω	-	vehicle turn rate
ϕ	-	vehicle bank angle

For the periodic trimming problem, the vehicle is said to be in trim if the time averaged flight paths over the partial period is equal to the stipulated values.

$$\overline{\mathbf{x}} = \mathbf{x}_t$$

Here, $\overline{\mathbf{x}}$ is the time averaged integral of the flight paths across the partial period t_p given by :-

$$\overline{\mathbf{x}} = \frac{1}{t_p}\int_0^{t_p} \mathbf{x}dt$$

$\mathbf{x}_t$ is the targeted values of $\mathbf{x}$ and $t_p = \frac{2\pi}{3\omega}$ is the partial period for a three blade rotor with angular velocity ω.

The PPTA is adopted and implemented for obtaining the trim solution of the tilt-wing model.

5 Flight Path Manoeuvring

The mathematical model described in the previous sections is formulated and implemented as forward simulation where vehicle response is the output and pilot control the input. However, a forward simulation model is inadequate in evaluating the capability of an aircraft to perform precisely defined manoeuvres. An alternative approach, known as inverse simulation, where the vehicle response is considered as the input and pilot control motions thought of as output is implemented for the tilt rotor/tilt wing aircraft

The algorithm for the inverse simulation of the tilt rotor/wing aircraft used in this work is based on the 'Genisa' algorithm [2] developed at the University of Glasgow for helicopter flight. The Genisa algorithm attempts to find the control displacements $\mathbf{u}$ required to achieve the desired flight path at the next time step. In other words the algorithm looks for a solution $\mathbf{u}(t_k)$ at the k-th time step which satisfy the following equation:-

$$\mathbf{e}(t_{k+1}) = \mathbf{Y}(t_{k+1}) - \mathbf{Y}_D(t_{k+1}) = 0 \qquad (1)$$

where $\mathbf{Y}$ and $\mathbf{Y}_D$ are respectively the actual and desired output vector and $\mathbf{e}$ is the error vector. The output vector $\mathbf{Y}(t_{k+1})$ can be expressed as a function of the state variables $\mathbf{X}(t_{k+1})$ i.e,

$$\mathbf{Y}(t_{k+1}) = g\left(\mathbf{X}(t_{k+1})\right) \qquad (2)$$

The state variable $\mathbf{X}(t_{k+1})$ at the $k+1$-th time step is obtained by integrating:-

$$\mathbf{X}(t_{k+1}) = \int_{t_k}^{t_{k+1}} \dot{\mathbf{X}}(t_k)dt + \mathbf{X}(t_k) \qquad (3)$$

where derivatives $\dot{\mathbf{X}}(t_k)$ of the state vector can be expressed as functions of the state vector $\mathbf{X}(t_k)$, the current approximation of the control vector $\mathbf{u}(t_k)$ and time t_k:

$$\dot{\mathbf{X}}(t_k) = f(\mathbf{X}(t_k), \mathbf{u}(t_k), t_k)$$

The algorithm starts at $t = 0$ with trim values as the initial guess for $\mathbf{u}(0)$ and the equations of motion are integrated to obtain the value of the state vector and there by output vector at the next time step. Newton-Raphson iterative scheme is used for solving equation 1 to obtain the value of $\mathbf{u}(0)$. The iteration is continued until the error vector is less than the tolerance limit and moved forward to the next time step to obtain a time history of control displacements required to guide the aircraft through the desired flight path represented by $\mathbf{Y}_D$.

5.1 Definition of the output vector

From a mathematical point of view, a flying task can be represented in terms of the three spatial co-ordinates of the locus of the aircraft centre of mass relative to an earth fixed frame. Since a tilt rotor/wing aircraft has five control inputs in helicopter mode flight, it is possible to add two more components to the output vector. A natural choice for the additional two output components are the Euler angles which represent the orientation of the aircraft while performing a flying task. Hence, a general output vector for the tilt rotor/wing inverse simulation can be written as:

$$\mathbf{Y} = \begin{bmatrix} x_e \\ y_e \\ z_e \\ \phi \\ \psi \end{bmatrix} \qquad (4)$$

Here (x_e, y_e, z_e) are the earth fixed co-ordinates of the aircraft centre of mass, ϕ and ψ are the roll and heading angles of the aircraft. At this point it may be worthwhile to point out that it is not

always possible to constrain both ϕ and ψ(e.g, in an aggressive lateral manoeuvre). In such cases one of the five controls is made redundant and only one of the two Euler angles is constrained. Also, during a conversion and aeroplane mode flight with shaft angles(γ) greater than 15 degrees there are only four controls available and hence the size of the output vector is to be restricted to four.

From a numerical point of view, specifying output vector in terms of the displacements can lead to numerical instabilities and there-by failure of the algorithm in cases of inverse simulation with too small or too large step lengths. The work done by Rutherford and Thomson [2] have shown that the instabilities can be eliminated by specifying velocities or acceleration profiles of the flight path rather than displacements. This offers no particular disadvantage as the velocity and acceleration profiles can readily be obtained by appropriate differentiations displacement profiles.

5.2 Mathematical Description of Flight Paths

A series of Mission Task Elements(MTE) are defined by the U.S. military to assess the handling qualities of rotorcraft[10]. These MTE are chosen to represent the flying missions likely to be under taken by the aircraft in its operational role. Mathematical representations of many of these MTEs have been developed at the University of Glasgow [11] as part of the research on helicopter handling qualities. A subset of the MTEs has been chosen in this work with the following objectives:-

1. To verify the use of inverse simulation for tilt rotor/wing application
2. Demonstrate the ability of a tilt rotor/wing aircraft to perform precisely defined manoeuvre.
3. Evaluate a comparative performance between a tilt rotor and a tilt wing aircraft.

Inverse simulation used in this work is limited to checking whether the aircraft can fly manoeuvre with out exceeding the control and power limits. Evaluation of the handling qualities of the aircraft is not addressed or incorporated in the model. The chosen manoeuvres and the tilt wing response are given in the following sub sections.

5.3 Rapid Slalom

A slalom in the earth x-y plane is one of the most widely used manoeuvre to demonstrate the lateral manoeuvrability of an aircraft. Track of a typical slalom in the earth x-y plane is shown in the Figure 3. A mathematical representation of it can be

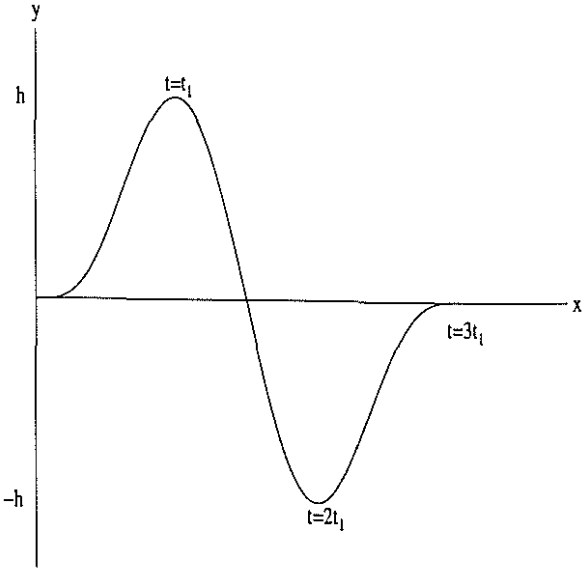

Figure 3: Earth x-y track of the slalom

obtained by considering following boundary conditions on the lateral displacement[11].

$$\begin{aligned} t = 0, &\quad y_e = 0, &\quad \dot{y}_e = 0, &\quad \ddot{y}_e = 0 \\ t = t_1, &\quad y_e = h, &\quad \dot{y}_e = 0 & \\ t = 2t_1, &\quad y_e = -h, &\quad \dot{y}_e = 0 & \\ t = 3t_1, &\quad y_e = 0, &\quad \dot{y}_e = 0, &\quad \ddot{y}_e = 0 \end{aligned}$$

where h is the maximum lateral displacement. A simple form satisfying the above boundary conditions is the 8th order polynomial:

$$\begin{aligned} y_e(t) = \quad & \left[-2\left(\frac{t}{t_1}\right)^9 + 27\left(\frac{t}{t_1}\right)^8 - \right. \\ & 144\left(\frac{t}{t_1}\right)^7 + 378\left(\frac{t}{t_1}\right)^6 - \\ & \left. 486\left(\frac{t}{t_1}\right)^5 + 243\left(\frac{t}{t_1}\right)^4 \right] \frac{h}{16} \end{aligned}$$

This polynomial can be readily differentiated to obtain the velocity in the earth axis y-direction. Assuming constant altitude and flight speed, velocities in the x and z direction can be obtained as:-

$$\begin{aligned} \dot{x}_e &= \sqrt{V_f^2 - \dot{y}_e^2} \\ \dot{z}_e &= 0 \end{aligned}$$

5.3.1 Slalom with zero banking and heading: In addition to the three velocity components in the earth axes, the bank angle ϕ and

the heading angle ψ are both constrained to zero. A slalom can be performed in this manner on a tilt rotor/wing aircraft due to the availability of two controls viz., θ_{0d} and θ_{1cc} in the lateral direction. The combination of combined lateral cyclic and differential collective input generate a net force in the desired y-direction and a net zero rolling moment making the aircraft to slide slip with out banking. Referring to the Figure 4 it can be seen that the rolling moment created by the combined lateral cyclic input is balanced by a negative input of differential collective. Differential collective input applied to the left and the right rotors create an unbalanced yaw moment about vehicle C.G. This unbalanced yaw moment is balanced by the application of the differential longitudinal control input. The severity of the slalom performed with out banking and yaw is restricted due to the lack of available control power about the yaw axes(pedal input). Also, the vehicle seems to enter pitch instabilities(Figure 5) leading to the failure of the algorithm.

5.3.2 Slalom with zero heading: The inverse simulation results are given in Figures 6 and 7. In addition to the three velocity components in the earth axes, the heading angle ψ is constrained to zero. Since there are only four constraints, one of the controls viz., differential collective is made redundant during the inverse simulation. The manoeuvre is mainly driven by the combined lateral cyclic control input. It was found that inverse simulation failed to converge when attempting to perform on aggressive slalom with the combined lateral cyclic input made redundant. This is due to the unbalanced yaw moment generated as result of the differential collective on the rotors and the unavailability of sufficient control power in the yaw axes to keep the aircraft in zero heading.

5.4 Side step

A simple representation of the side step manoeuvre can be obtained by considering an acceleration from the hover to some maximum velocity in the lateral direction followed by a deceleration to the hover. The following expression for the velocity profile can be obtained by considering smooth entry and exit boundary condition and assuming v_m, the maximum velocity in the lateral direction, is reached half the way through the manoeuvre time t_m.

$$\dot{y}_e(t) = -64v_m\left[\left(\frac{t}{t_m}\right)^3 - 3\left(\frac{t}{t_m}\right)^2 + 3\left(\frac{t}{t_m}\right) - 1\right]\left(\frac{t}{t_m}\right)^3$$

In a manner similar to the slalom the side step can be performed either with or with out banking - heading being constrained to zero in both cases. As stated before the aggression level of side step with out heading and banking is restricted due to yaw control power limit. The maximum velocity that could be achieved was found to be 4 Knots for both the configurations. The control history of the side step is given in Figure 8.

More aggressive side steps can be performed by allowing the bank angle to change and the differential collective input made redundant. A control history of a side step with v_m=10 Knots is given in Figure 10. Once again the aggression level is restricted by the extensive yaw moment created by the vertical fin.

5.5 The Hurdle-hop Manoeuvre

This is a purely longitudinal manoeuvre in which the pilot has to clear an obstacle of height h in time t_m and return to initial altitude. The maximum height is assumed at the mid point of the manoeuvre. A 6th order polynomial curve representing the altitude profile which also satisfies the smooth entry and exit condition for the hurdle-hop is given below:-

$$z_e(t) = 64h\left[\left(\frac{t}{t_m}\right)^3 - 3\left(\frac{t}{t_m}\right)^2 + 3\left(\frac{t}{t_m}\right) - 1\right]\left(\frac{t}{t_m}\right)^3$$

If constant flight speed and zero lateral velocity are assumed:-

$$\dot{x}_e = \sqrt{V_f^2 - \dot{z}_e^2}$$
$$\dot{y}_e = 0$$

Since the hurdle-hop is assumed to be performed in helicopter mode there are five controls available and hence the roll angle ϕ and the heading ψ can be constrained to zero.

The control history and the vehicle response for a hurdle-hop manoeuvre of height 30 meters are shown in Figure 12. Since the manoeuvre is purely longitudinal only longitudinal controls are used.

The altitude profile is maintained by the the combined collective - the longitudinal stick keeping the flight speed constant.

6 Comparison of Tilt Wing and Tilt Rotor

The tilt wing and tilt the tilt rotor simulation programme are run to obtain a comparison of the performance of both the configurations and are given in Figures 13 to 18.

6.1 Trim map

The partial periodic trimming algorithm is used to generate a series of trim solutions for conditions of level flight (zero side slip, angle of climb, turn rate and roll) for shaft angles ranging from 0 degree to 90 degree in steps of 5 degree. At every step of the shaft tilt angle PPTA is run from 0 to 400 Knots to obtain a lower and an upper limit on the speed at which the vehicle can be flown in level trim. These lower and upper limit are plotted against the shaft angle to obtain a $\gamma - V_f$ envelope through which the aircraft can be transitioned from the helicopter mode to the aircraft mode flight. The trim map thus obtained for tilt wing and tilt rotor aircraft are shown in Figures 13 and 14. It can be seen that the tilt rotor has a larger range of flight speeds at which trim solution are found with the most critical shaft angles being between 60 and 75 degree for the tilt wing. For the tilt wing configuration as the wing/shaft assembly is tilted forward the angle of attack of the wing passes through stall and post stall regimes. For shaft tilt angles below 60 degree the vertical component of the rotor thrust provides sufficient lift. The contribution of lift from the rotor reduces as the shaft angle is incresed beyond 60 degrees. The criticality between 65 degrees and 75 degrees is due to the fact that at these shaft angles, the wing operates at angles of attack in the stalling region producing reduced lift. The wing starts to produce adequate lift after about 75 degrees and hence a wider range of flight speed above some minimum speed. The maximum speed achieved by the tilt wing configuration in helicopter and conversion mode flight was lower than the tilt rotor due to the high angle of attack of the tilt wing compared to the tilt rotor-which has its wing in the horizontal position in all flight modes. Trim solutions were obtained for both the configurations in aeroplane mode flight(shaft tilt angles more than 80 degree) at flight speeds higher than 400 Knots although in practice this is not possible. There being no engine model in the simulation, the maximum speed is limited only by the control power available. The upper limit on flight speed achieved by the simulation model will not represent the real situation due to the limitations of the level of sophistication incorporated in the mathematical model.

6.2 Conversion from helicopter to aeroplane mode

Conversion from helicopter to aeroplane mode flight were performed for both the configurations using a control map generated by PPTA at discrete shaft tilt positions ranging from 0 to 90 degree. The conversion manoeuvre is divided into discrete points at different shaft tilt angles. The trimming algorithm is then applied to obtain the necessary control inputs for attaining level trim at these shaft tilt positions. The control inputs are then linked together to form a history(control map) which is used drive the vehicle along the required path during the transition. A fifth order polynomial which ensures smooth boundary conditions at the beginning and at the end of the conversion is used to define the profile of the tilt angle (Figure 15). The flight speed is linearly increased from 40 Knots at 0 degree shaft tilt to 120 Knots at 90 degree shaft tilt(Figure 15) with the conditions of level flight. The control maps of a 15 seconds conversion from 0 degree to 90 degree shaft tilt for both the configurations are shown in Figure 16. The control inputs at the time points of the forward simulation of the transition are obtained from linear interpolation of the discrete control map values. With reference to the transition time histories of the flight paths (Figures 17 and 18), it can be seen that the specified linear increase of the flight speed from 40 Knots to 120 Knots is achieved by both the configurations, with a small heavily damped oscillation towards the end of the transition. Zero angles of climb are not maintained through most of the conversion even though the control inputs represent steady state trim values for zero angle of climb. The maximum descent angle reached for the tilt wing configuration is about 15 degree and about 5 degree for the tilt rotor configuration.

6.3 Comparison of thrust and torque requirements

The sum of the left and the right rotor torque and thrust in hover for both the configurations at three shaft tilt positions (5, 20 and 45 degrees) are given in Figures 19 and 20. Figure 19 shows that the tilt rotor configuration requires about 18% more torque(and hence power) compared to the equivalent tilt wing configuration. The increased torque requirement is attributed to the higher collective input due to the down wash of rotor inflow on to the

tilt rotor wing. The higher collective input result in an increased drag on the rotor blades and thereby a greater requirement of engine torque. The effect of rotor down wash on the tilt rotor is more evident in the plot of the thrust - the tilt rotor configuration requiring about 12% more.

6.4 Comparison of controls

The combined collective and longitudinal stick position to produce trimmed level flight at four different shaft tilt position are given in Figures 21 and 22. Up to about 40 Knots the collective input of the tilt rotor configuration is higher than the tilt wing due to the adverse effect of rotor down wash on to the tilt rotor wing. At speeds above 40 Knots the increased aerodynamic drag on the wing of the tilt wing configuration starts to offset the rotor down wash advantage causing higher collective input. As the shaft angle is increased beyond 60 degrees the effect of rotor down wash on the tilt rotor become less significant resulting in less collective input than the tilt wing for the whole range of flight speed.

In helicopter mode the vehicle speed is increased by orienting the thrust vector forward by applying a positive(forward) input to the combined longitudinal cyclic as shown in Figure 22. The forward input of longitudinal cyclic has a secondary effect of generating a nose down pitching moment causing the vehicle to pitch down with increasing flight speed (Figure 23). When the thrust vector is oriented forwards their vertical component decreases and consequently more collective is required to balance the vehicle weight. The initial dip in the collective input requirement for both the configurations is due to the increased rotor efficiency as the vehicle comes out of hover. The collective input starts to increase again as the vehicle moves faster due to higher aerodynamic drag and change in the orientation of the thrust vector.

The maximum speed achieved by the tilt wing configuration in helicopter mode flight was considerably lower than the tilt rotor configuration. The main reason for this is that at the same speed the tilt wing pitches down more than the tilt rotor to overcome the higher wing drag requiring a greater value of combined longitudinal cyclic leading to control limiting.

The pitch equilibrium and the control requirements of both configurations at two different flight speeds for varying shaft tilt positions are given Figures 24 to 26. From the plot of the pitch attitude it can be seen that vehicles adopt greater nose up attitude as the tilt angle is increased from the helicopter mode to the aeroplane mode. In the case of the tilt rotor configuration, the collective input at 70 Knots flight tends to reduce initially as the shaft is tilted forward. The reason for this is that the increased angle of attack(due to the higher pitch attitude) generates higher wing lift reducing the thrust requirement from the rotors. As the shaft is tilted further the angle of attack is increased so that the wing enters the non-linear region and produce lesser lift. This is the reason for the increase of collective input beyond a shaft tilt of about 30 degree. At lower speeds(5 Knots) the collective input requirement reduces with the increase of shaft tilt angle due to the diminished influence of rotor down wash.

For the tilt wing configuration the collective input is flatter because the wing is tilted along with the rotor shaft and hence there is very little change in the angle of attack.

7 Conclusions

1. A mathematical model of a tilt wing configuration has been developed based on an equivalent tilt rotor simulation model. The tilt rotor and the tilt wing model assumed to have the same aerodynamic configurations as that of the XV15 tilt rotor. Both the configurations employed same control authority i.e, rotor cyclic blade controls in helicopter and transition mode flights and conventional fixed wing aerodynamic control surfaces in aeroplane mode. The mathematical model consisted of a blade element rotor model with dynamic inflow . Aerodynamic look up tables were used to evaluate the vehicle aerodynamics including wing, fuselage, horizontal stabiliser and vertical fins. Rotor wake impingement on the wing and horizontal stabiliser has been included and found to have significant effect on the vehicle dynamics.

2. The partial periodic trimming algorithm by Bradley and McVicar [8] was extended to the tilt wing model. The trimming algorithm has been found to produce trim solutions in helicopter, conversion and aeroplane mode flights. The PPTA is used to generate a series of trim solutions to obtain a control map which is used to transit the tilt wing aircraft from helicopter mode to aeroplane mode.

3. Manoeuvre guidance capability of the tilt

wing configuration is evaluated using the method of inverse simulation. For this the 'Genisa' algorithm by Rutherford and Thomson [2] is implemented for the tilt wing application. Using the inverse simulation technique the tilt wing was flown precisely defined representative manoeuvres in the lateral and longitudinal directions. It was found that the tilt wing configuration can perform slalom and side step manoeuvres like a conventional helicopter to a lesser aggression level. Also, unlike a helicopter the tilt wing configuration could perform a lateral manoeuvre with zero bank and heading angles. The aggression level in the lateral direction was limited mainly due to the high value of yaw moment created by the vertical fin positioned at the vehicle empennage. Combined lateral cyclic input was found to be more effective than the differential collective in achieving lateral movements. This was due to the unbalanced yaw moment created about the vehicle centre of gravity when different collective inputs were applied to the left and right rotors.

4. A comparative study of the flight dynamics of equivalent tilt rotor and tilt wing configurations was performed. For both the configurations, a trim map of shaft tilt angle and flight speed were obtained within which trim conditions of zero side slip, angle of climb, turn rate and roll were satisfied. The tilt rotor configuration was found to have a wider range of flight speeds for all shaft tilt angle up to 80 degrees at which trim solutions were obtained. At lower shaft angles(helicopter mode) maximum attained speed for the tilt wing configuration was about 70 Knots. This is because of the higher aerodynamic drag generated by the wing in the vertical orientation. At shaft angles between 65 and 75 degrees tilt wing was found to have a narrow range of flight speeds at which trim solutions were obtained. This was because at these shaft tilt angles the tilt wing operate in the non-linear region of the lift curve.

   During a conversion from the helicopter mode to the aeroplane mode flight both the configurations approximately followed the specified flight paths with the exception of climb angle. The maximum deviation of climb angle from the specified zero value was 15 degrees descent for the tilt wing and 20 degree ascend for the tilt rotor.

   Down load due to rotor inflow in hover was about 12% more for the tilt rotor configuration, effectively reducing the gross lift. This loss in lift amounts to about 18% more total engine torque requirement for the tilt rotor in hover.

8 Limitation and Future Work

The main limitation of this work are summarised below.

1. Model sophistication within the scope of flight mechanics analysis.
   - Constant rotor speed is assumed for forward and inverse simulations.
   - Aerodynamic interaction between the vehicle components are modelled in a rudimentary manner.
2. Wing stall during a tilt wing conversion is not adequately modelled although non-linear lift and drag coefficients look-up tables are provided for the complete range of angles of attack.
3. Wing trailing edge flap settings are changed as function of shaft tilt angle for the tilt wing conversion schedule and found to offer no particular advantage though most tilt wing models in the past used flap control [12] programs in conversion. This may be due to the aerodynamic characteristics of the XV-15 wing which is optimised for tilt rotor application. However, this aspect needs to be investigated further.
4. The requirement for precise definitions of flight paths inhibits the application of inversion simulation for many cases of flight path manoeuvring. For example a conversion manoeuvre with a linear increase of flight speed lead to failure since the altitude cannot be constrained along with an increase in flight speed (at shaft tilt angle is more than 60 degree). A pilot model with error feed back based on a linear model is to be developed for the tilt rotor/tilt wing application.

References

[1] McVicar, J.S.G., *A Generic Tilt-rotor Simulation Model with Parallel Implementation*, Ph.D. Theses, University of Glasgow, Department of Aerospace Engineering, February 1993.

[2] Rutherford, S., Thomson, D.G., *Improved Methodology for Inverse Simulation*, Aeronautical Journal, March 1996, pp 79-86.

[3] Michael, J., Hirschberg, A., *V/STOL: The First Half Century*, Vertiflite, Volume 43, Number 2, March/April 1997, pp 34-54.

[4] Ishida, T., Nakatani, I., *TW-68 Tilt Wing High Speed Commercial VTOL* Vertiflite, Volume 36, Number 1, January/February 1990, pp 47-49.

[5] Chana, W.F., Sullivan T.M., *The Tilt Wing Advantage - for High Speed VSTOL Aircraft*, SAE Aerotech, Anaheim, October 1997.

[6] Padfield, G.D., *Helicopter Flight Dynamics*, Blackwell Science Ltd., 1996.

[7] Peters, D.A., HaQuang, N., *Dynamic Inflow for Practical Applications*, Journal of the American Helicopter Society, Technical Note, October 1988.

[8] McVicar, J.S.G., Bradley, R., *Efficient and robust algorithm for trim and stability analysis of advanced rotor craft simulations*, Aeronautical Journal, October 1997, pp 375-386.

[9] Harendra, P.B., et al, *A Mathematical Model for Real Time Flight Simulation of the Bell Model 301 Tilt Rotor Research Aircraft*, Bell Helicopter Company Report, No. 301-099-001, April 1973.

[10] Anon, *Aeronautical Description Standard ADS-33D-Handling Qualities Requirements for Military Rotorcraft*, US Army ATCOM, August 1994.

[11] Thomson, D.G., Bradley, R., *Mathematical Definition of Helicopter Manoeuvres*, Department of Aerospace Engineering, University of Glasgow, Internal Report, No. 9225.1992.

[12] Pegg, R.J., Kelly, H.L., Reeder, J.P., *Flight Investigation of the VZ-2 Tilt-Wing Aircraft with Full-Span Flap*, NASA Technical Note, NASA TN D-2680, March 1965.

Inverse Simulation of Tilt wing - Heading and Banking Constrained 15 Meter Slalom Performed at 30 Knots Speed

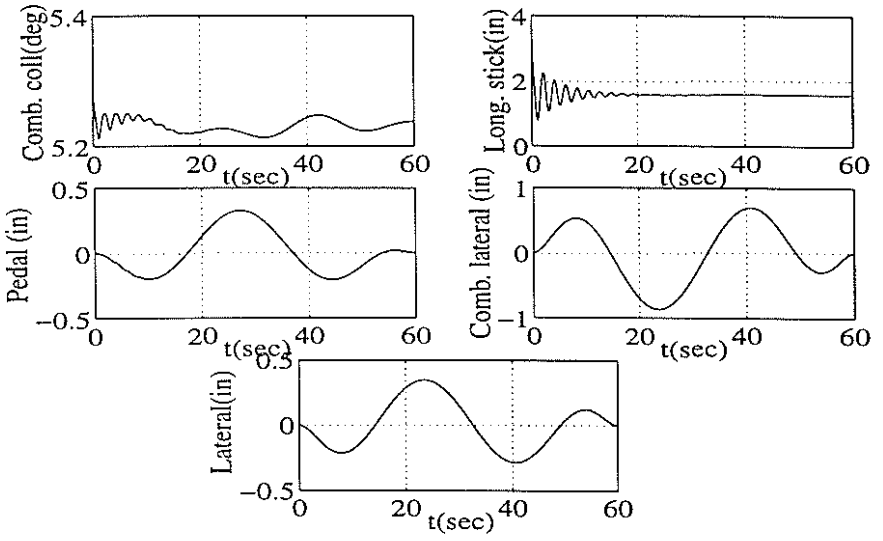

Figure 4: Tilt wing control history for heading and banking constrained slalom

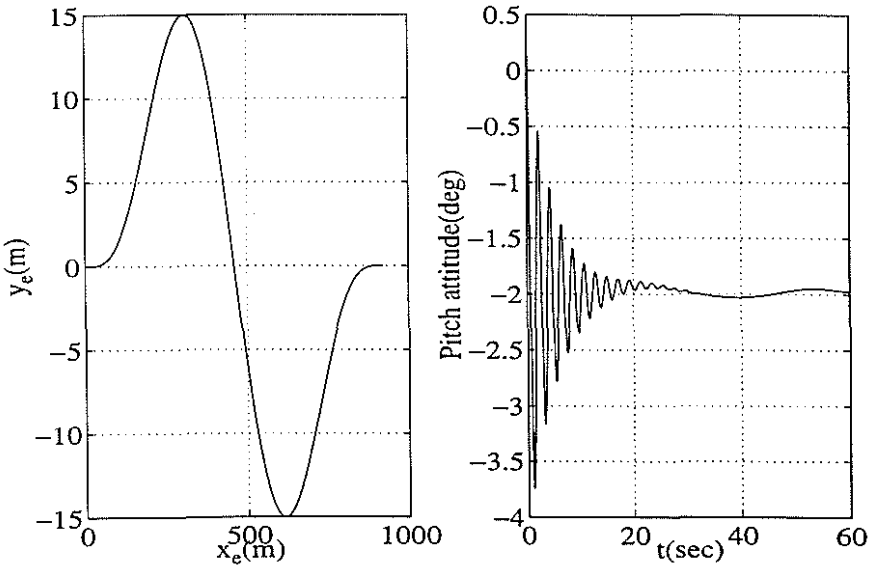

Figure 5: Vehicle response during the heading and banking constrained slalom

Inverse Simulation of Tilt wing - Heading Constrained 30 Meter Slalom Performed at 30 Knots Speed

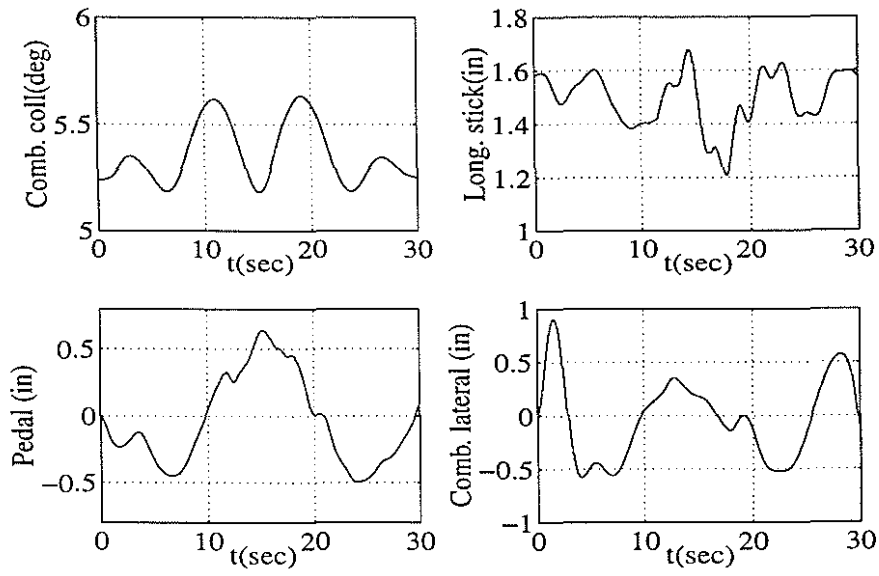

Figure 6: Tilt wing control history for heading constrained slalom

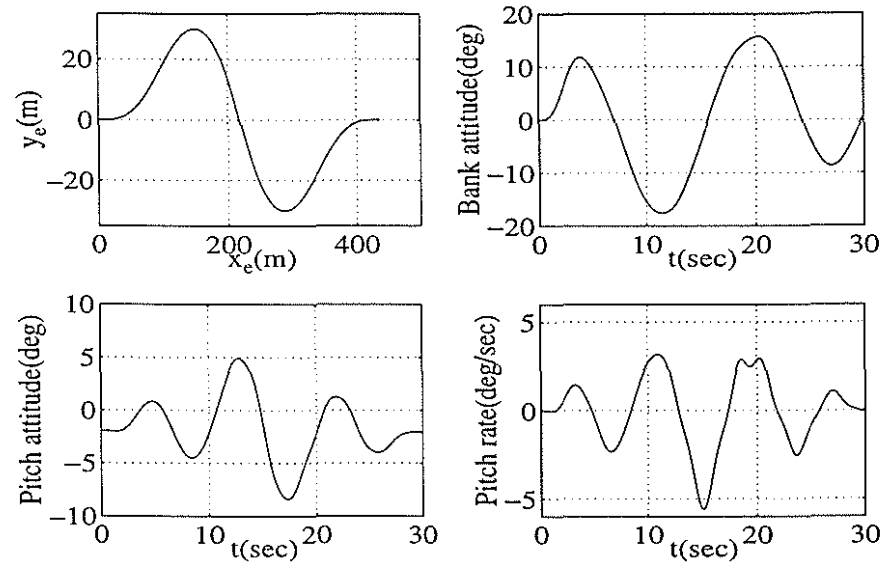

Figure 7: Vehicle response during the heading constrained slalom

Inverse Simulation of Tilt wing - Heading Constrained and Banking Side Step with Maximum Lateral Velocity 3 Knots

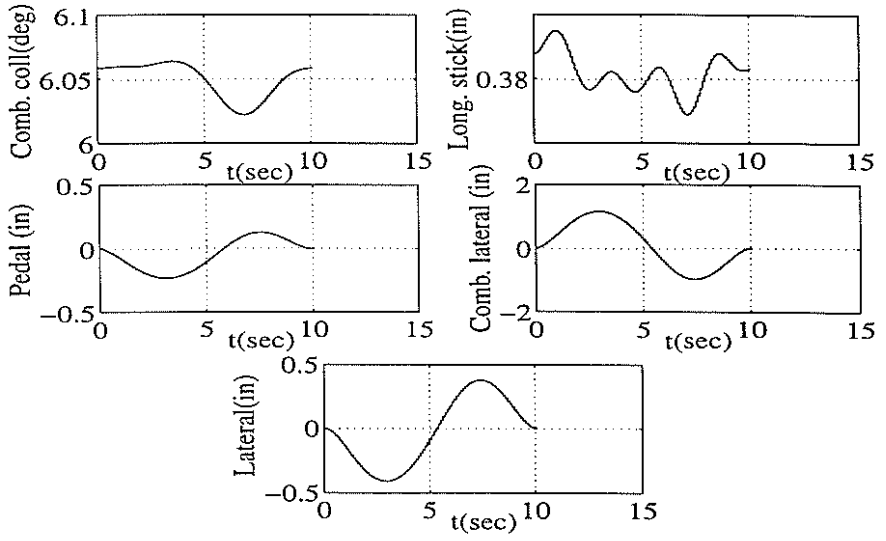

Figure 8: Tilt wing control history for heading and banking constrained side step

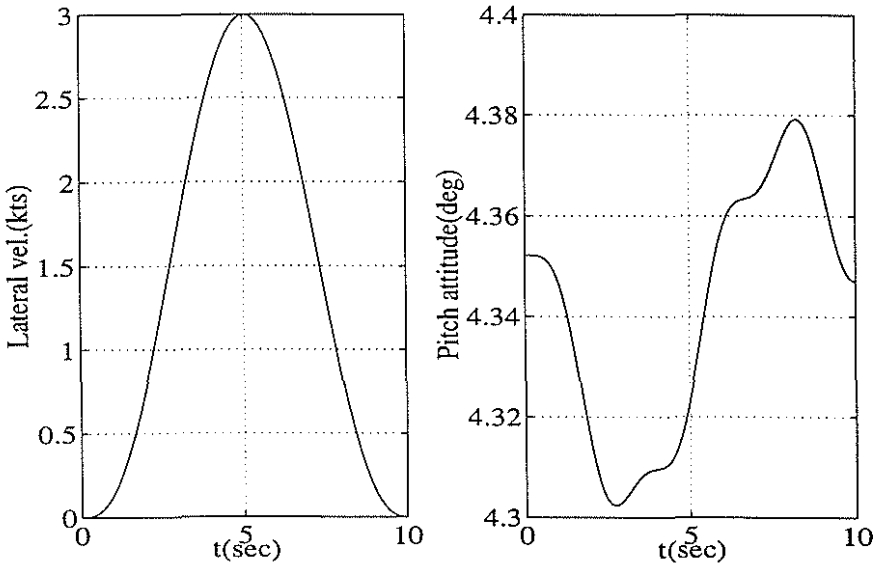

Figure 9: Vehicle response during the heading and banking constrained side step

Inverse Simulation of Tilt wing - Heading Constrained Side Step with Maximum Lateral Velocity 10 Knots

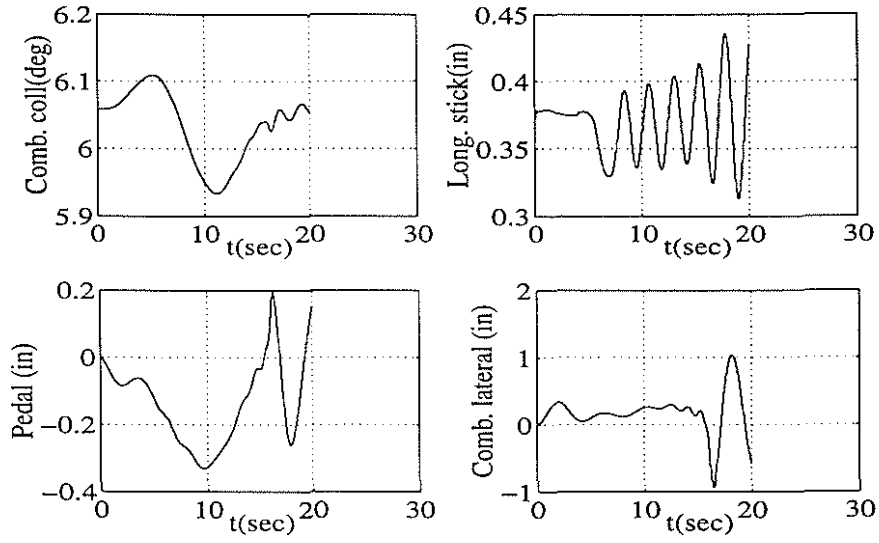

Figure 10: Tilt wing control history for heading constrained side step

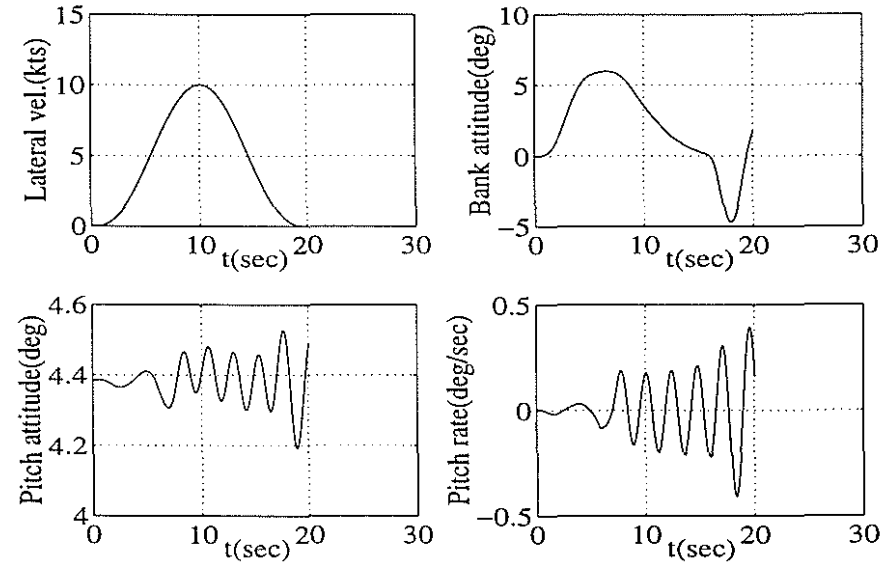

Figure 11: Vehicle response during the heading constrained side step

Inverse Simulation of Tilt wing - Heading and Banking Constrained Hurdle Hop Manoeuvre of Height 30 Meter

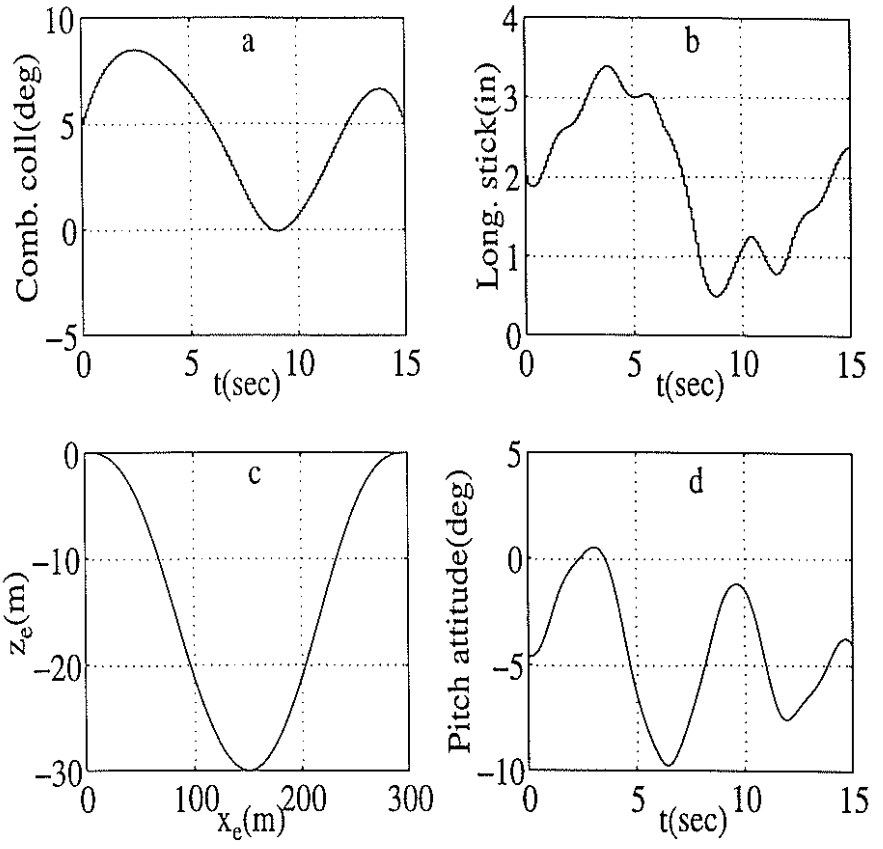

Figure 12: Tilt wing control history for heading and banking constrained side step

Trim Map of Tilt Wing and Tilt Rotor

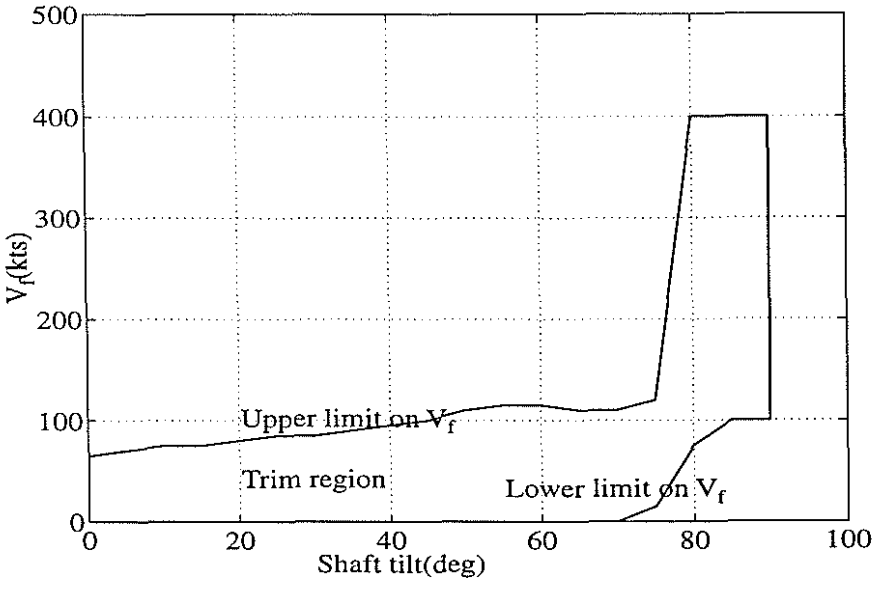

Figure 13: Trim Map of Tilt Wing

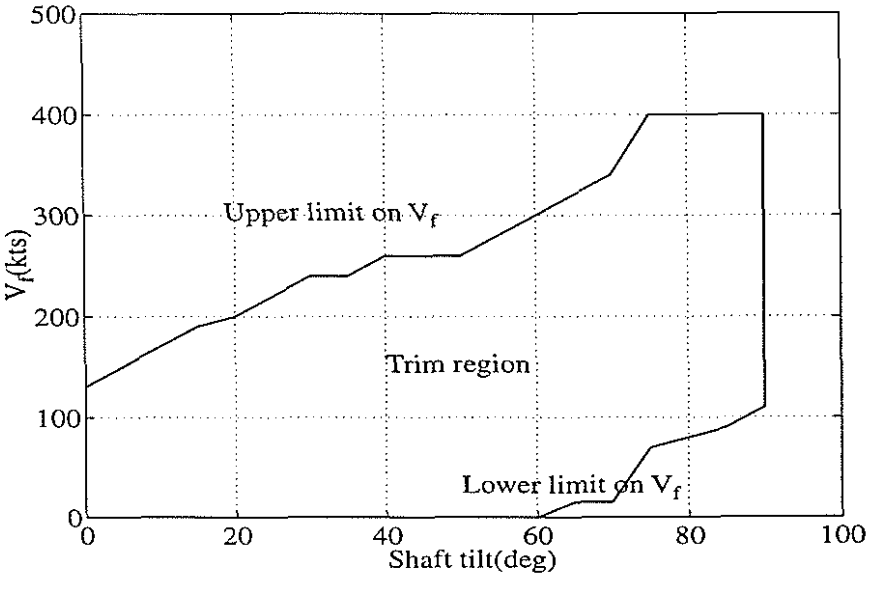

Figure 14: Trim Map of Tilt Rotor

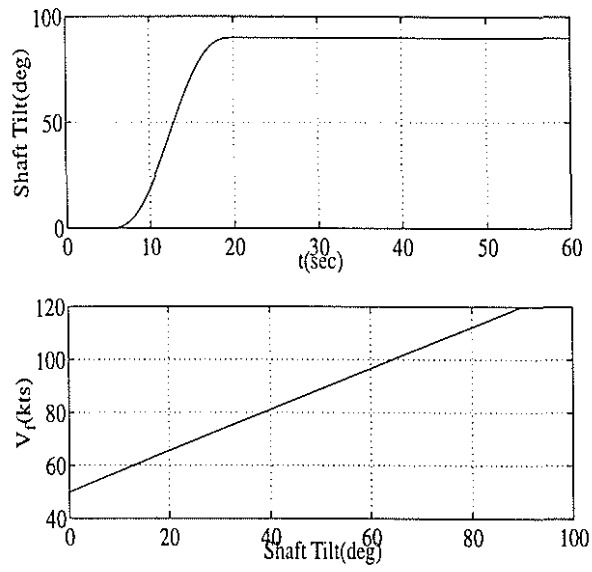

Figure 15: Specified shaft tilt and flight speed during conversion

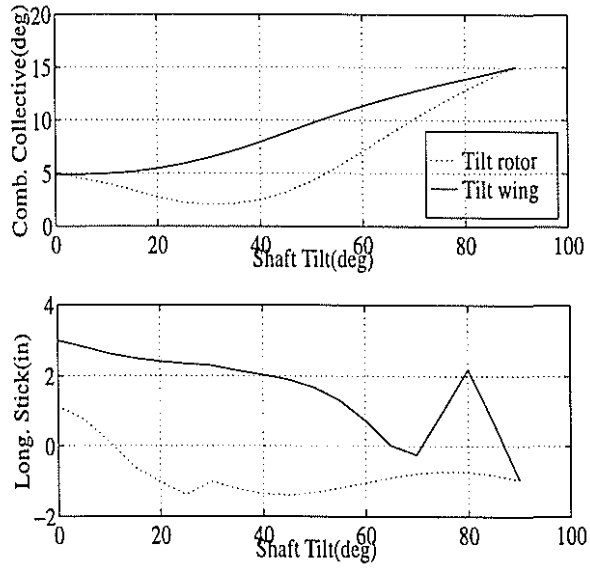

Figure 16: Controls for trim at different shaft tilt angles

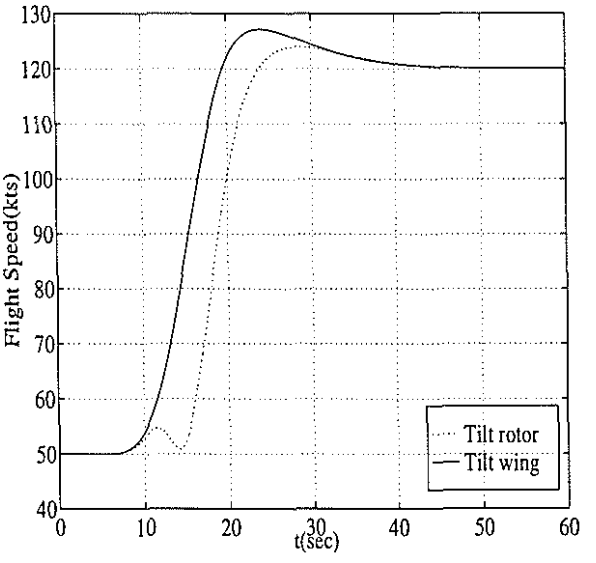

Figure 17: Flight speed adopted during conversion

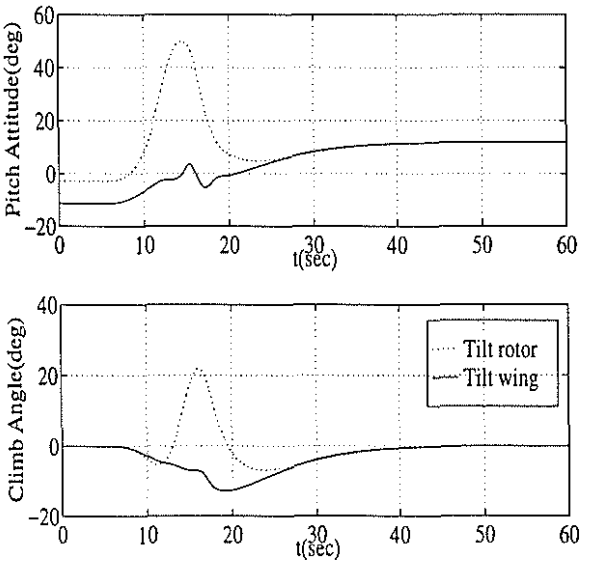

Figure 18: Pitch and climb angle adopted during conversion

Tilt Wing and Tilt Rotor Torque and Thrust in Hover

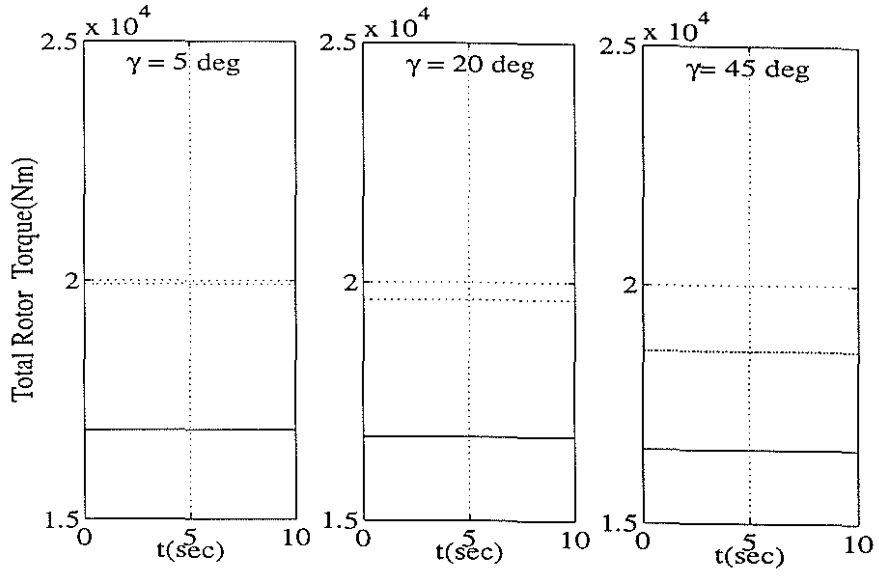

Figure 19: Rotor 1 + Rotor 2 torque for tilt wing and tilt rotor in trimmed hover

— Tilt Wing
.... Tilt Rotor

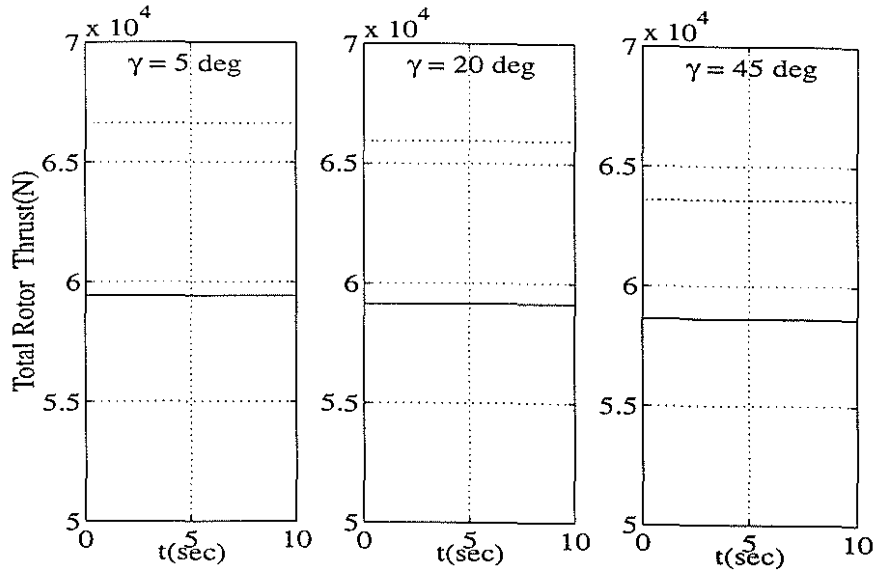

Figure 20: Rotor 1 + Rotor 2 thrust for tilt wing and tilt rotor in trimmed hover

— Tilt Wing
.... Tilt Rotor

Control position with Varying Flight Speed

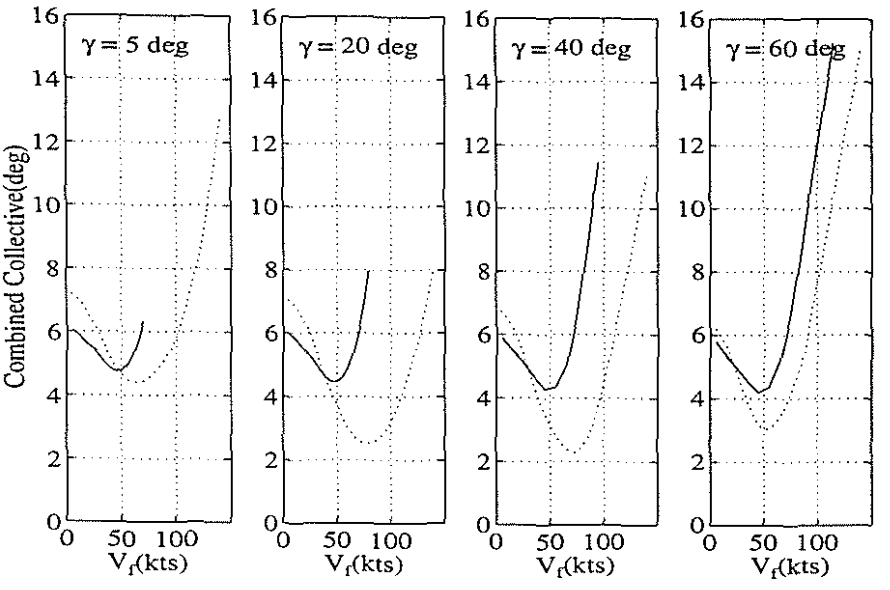

Figure 21: Combined Collective input for trim solutions with varying flight speed

— Tilt Wing
.... Tilt Rotor

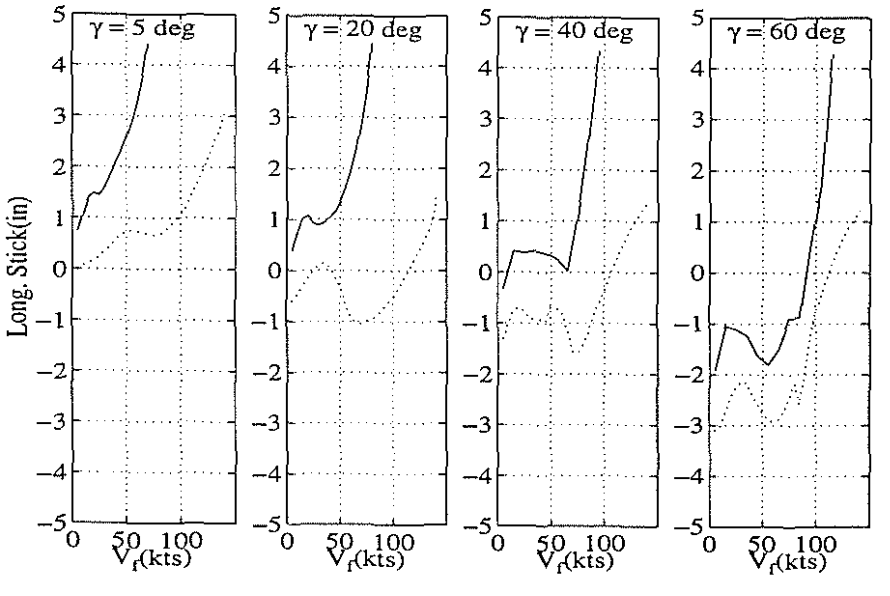

Figure 22: Long stick input for trim solutions with varying flight speed

— Tilt Wing
.... Tilt Rotor

Pitch Attitudes of Tilt Wing and Tilt Rotor

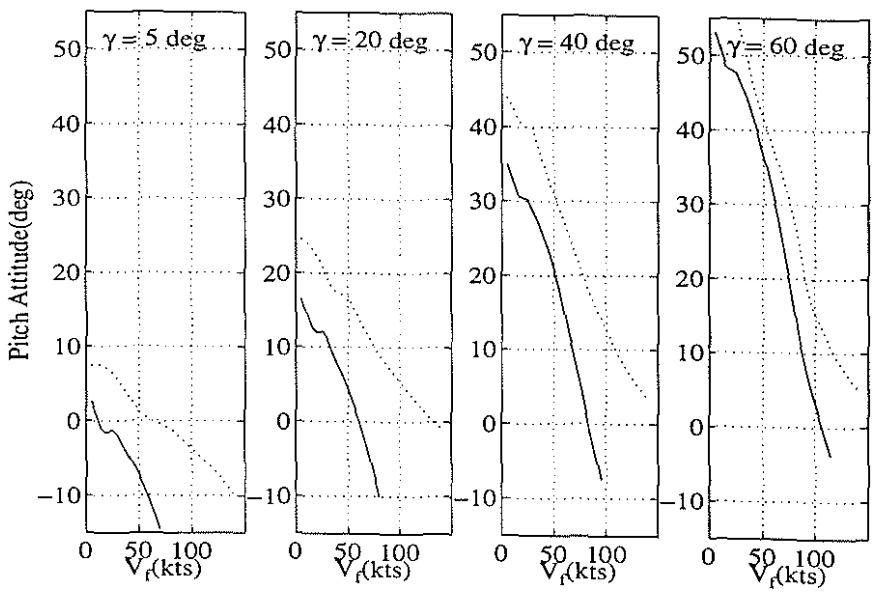

Figure 23: Pitch angle in trim solutions with varying flight speed

— Tilt Wing
.... Tilt Rotor

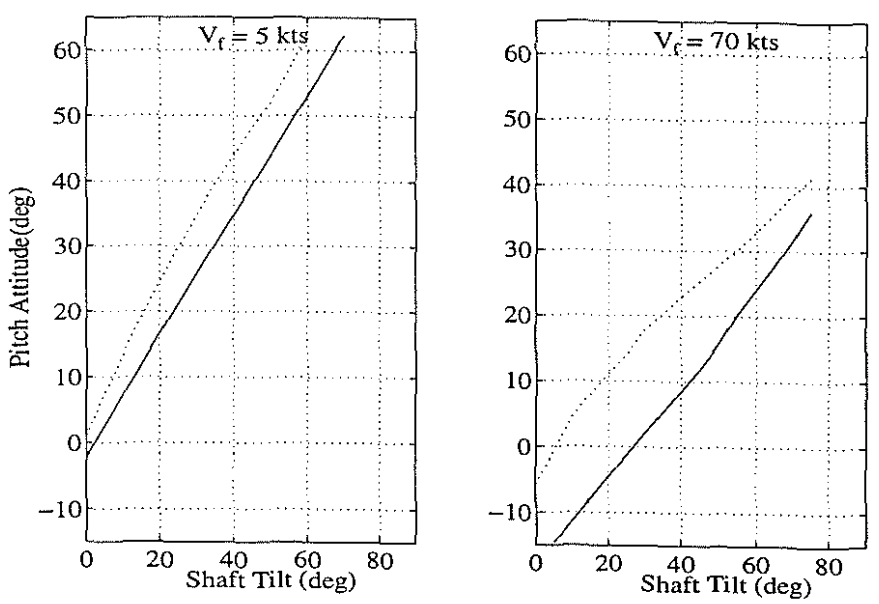

Figure 24: Pitch angle in trim solutions with varying shaft tilt

— Tilt Wing
.... Tilt Rotor

Control position with Varying Shaft Tilt

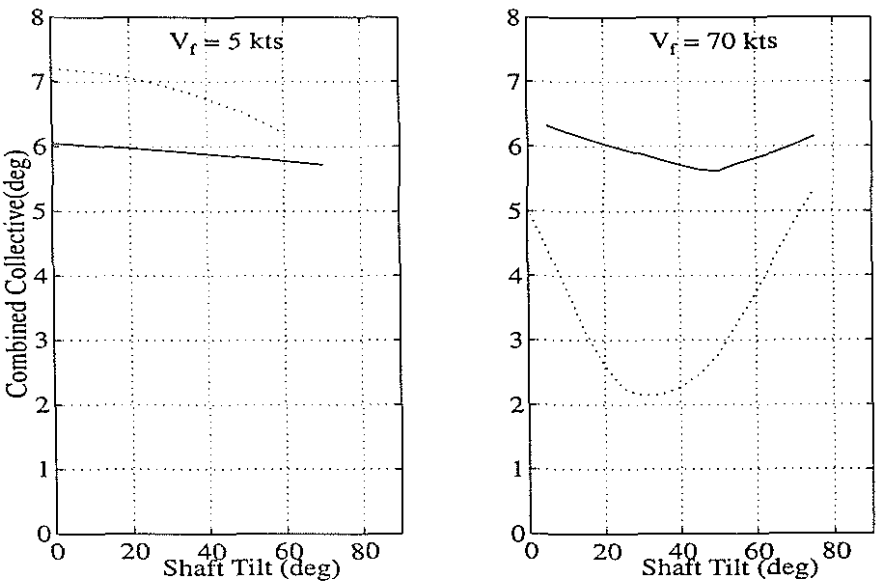

Figure 25: Combined Collective input for trim solutions with varying shaft tilt

— Tilt Wing
.... Tilt Rotor

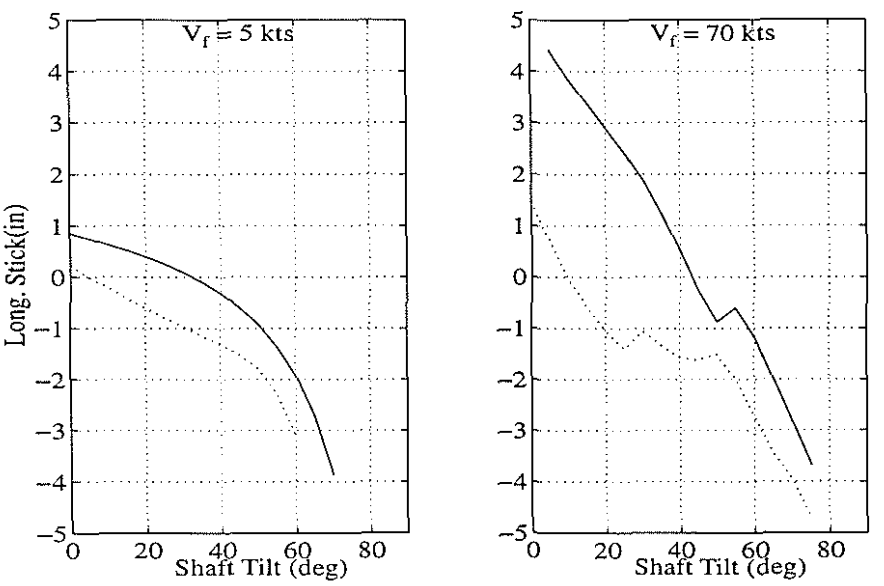

Figure 26: Long stick input for trim solutions with varying shaft tilt

— Tilt Wing
.... Tilt Rotor